JGR Biogeosciences

RESEARCH ARTICLE
10.1029/2020JG005851

Headwater Catchments Govern Biogeochemistry in America's Largest Free-Flowing River Network

David W. French[1], Daniel E. Schindler[1], Sean R. Brennan[1], and Diane Whited[2]

[1]School of Aquatic and Fishery Sciences, University of Washington, Seattle, WA, USA, [2]Flathead Lake Biological Station, University of Montana, Polson, MT, USA

Key Points:
- Little is known about the scales at which both watershed and instream factors shape streamwater biogeochemistry
- Headwater catchment conditions such as relief and geology are important drivers of streamwater constituents across a river network
- Conservative tracers such as calcium had stronger spatial autocorrelation than dissolved organic carbon and labile nutrients like nitrate

Supporting Information:
- Supporting Information S1

Correspondence to:
D. W. French,
dfrench@uw.edu

Citation:
French, D. W., Schindler, D. E., Brennan, S. R., & Whited, D. (2020). Headwater catchments govern biogeochemistry in America's largest free-flowing river network. *Journal of Geophysical Research: Biogeosciences*, *125*, e2020JG005851. https://doi.org/10.1029/2020JG005851

Received 17 MAY 2020
Accepted 3 NOV 2020
Accepted article online 21 NOV 2020

Abstract Riverine chemistry reflects both watershed conditions and instream processing, both of which vary across river networks, yet little is known about the scales at which watershed attributes regulate biogeochemical constituents. We used spatial stream network (SSN) models to quantify both watershed and instream effects on streamwater constituents in the Kuskokwim River (western Alaska), the largest free-flowing river in the United States. We assessed chemical constituents spanning from labile nutrients (nitrate [NO_3^-] and orthophosphate [PO_4^{3-}]) to biologically and chemically conservative tracers (calcium [Ca^{2+}], strontium [Sr^{2+}], and Sr isotopes [$^{87}Sr/^{86}Sr$]). We also examined the behavior of dissolved organic carbon (DOC) relative to these constituents to understand whether bulk DOC behaved conservatively in a large boreal river network, where future changes in DOC and nutrient loading are expected under a shifting climate. We derived watershed spatial covariates comprising land cover, geology, and geomorphic characteristics at 14 different spatial extents based on stream order and relative to position in the river network to understand the effect of distant and proximal watershed attributes on streamwater constituents. For all constituents but $^{87}Sr/^{86}Sr$, watershed attributes in low-order headwater catchments yielded the best predictive ability for streamwater constituent concentrations across the entire network. Spatial patterning for conservative tracers and bulk DOC showed strong spatial autocorrelation, whereas PO_4^{3-} and NO_3^- exhibited spatial patchiness indicative of instream processing. Our work shows that headwater streams are disproportionately important contributors to network-wide biogeochemical constituents supporting aquatic food webs and that conservation and management of aquatic systems should include these small and often remote watershed areas.

Plain Language Summary Streamwater chemistry is influenced by watershed attributes like geology, gradient, and land cover and biochemical changes occurring within the stream channel, but how the relative importance of these factors changes as water moves through a river network is not known. We used a statistical model that accounts for water flows and the spatial layout of the river to study how stream chemistry is influenced by both watershed attributes and instream conditions at local to watershed-wide scales. We studied the Kuskokwim River in Alaska, America's largest free-flowing river, and found that conditions in small, headwater streams play a disproportionately important role in shaping streamwater chemistry throughout the river network. We also found that chemicals that are rapidly used by algae and microbes are spatially more variable in the river network when compared to passively transported chemicals that have lower biological demand. This work is important because streamwater chemical patterns can influence how different organisms are distributed in rivers, and certain watershed attributes will influence how changing climate and land use affect river chemistry. Studying how different parts of the watershed influence streamwater chemistry will help scientists and resource managers understand how riverine chemistry and food webs may change in the future.

1. Introduction

Chemical conditions in rivers reflect both watershed attributes (Bormann & Likens, 1967) and instream processing (Webster & Patten, 1979). Streamwater constituents including dissolved organic carbon (DOC) and inorganic nutrients (e.g., nitrate [NO_3^-] and orthophosphate [PO_4^{3-}]) are key factors controlling the productivity of riverine food webs (Meyer et al., 1988). Spatial patterns in these constituents influence the distribution and productivity of aquatic biota and in turn biota can modify streamwater solute concentrations to downstream reaches (Meyer et al., 1988; Vannote et al., 1980). As water and its chemical constituents flow through dendritic river networks, processes of instream uptake and tributary mixing generate spatial

patterns in chemical conditions across the network. Understanding the balance of watershed versus instream factors shaping biogeochemical variability throughout river networks would improve our ability to manage the diverse conditions that support healthy aquatic ecosystems, yet relatively few studies have quantified how the spatial configuration of watershed attributes affects spatial patterning in stream chemistry (but see Abbott et al., 2018; Creed et al., 2015; Shogren et al., 2019; Zimmer et al., 2013) or have documented spatial patterns in chemical constituents that lie along a reactivity gradient (i.e., from labile nutrients to more conservative elements such as calcium, but see Likens & Buso, 2006; McGuire et al., 2014).

Streamwater constituents that have low biological demand (e.g., Sr^{2+} and calcium [Ca^{2+}]) or chemical reactivity generally behave as conservative indicators of watershed geophysical properties (Brennan et al., 2016; Hogan & Blum, 2003). Watershed attributes influencing streamwater chemistry include topography, geology, hydrology, land cover, and soil properties (Lintern et al., 2018), which vary across a range of spatial scales within watersheds. The influence of watershed attributes can be grouped broadly into three main effects: source variation (e.g., bedrock geology), mobilization constraints (e.g., weathering and solubility), and delivery to the river network (e.g., hydrologic connectivity) (Granger et al., 2010). Of these effects, source variation can be quantified using publicly available geospatial data sets, from which physical features that affect delivery processes (e.g., slope and connectivity) can also be inferred. For example, 70.5% of variation in Sr isotope ratios ($^{87}Sr/^{86}Sr$) in a large Alaska river network was explained using a spatial stream network (SSN) model with geologic cover, watershed relief, and historic glacial extents, and much of the additional variation (22.9%) was accounted for by spatial autocovariance associated with downstream transport and mixing of source waters (Brennan et al., 2016).

Instream processing of labile constituents may result in spatially patchy constituent concentrations that are difficult to quantify using watershed attributes alone (Gooseff et al., 2008; McGuire et al., 2014; Peterson et al., 2001). Nutrients like NO_3^- and PO_4^{3-} whose availability often limits biological activity in rivers have a wide range of uptake lengths (0.08–4.92 and 0.02–61 km, respectively), which generally increase with stream order (Ensign & Doyle, 2006). Streams with rapid nutrient uptake tend to exhibit stronger spatial autocorrelation in concentrations at fine spatial scales and random or patchy autocorrelation at broader scales (Dent & Grimm, 1999; McGuire et al., 2014; Peterson et al., 2001). This fine-scale heterogeneity is governed by numerous factors, including constituent concentration (Casas-Ruiz et al., 2017; Teodoru et al., 2009), leaching or decomposition (Kaplan & Bott, 1982; Meyer, 1990), diel changes in algal production or microbial transformations (Jankowski & Schindler, 2019; Kaplan & Bott, 1982), photolysis (Blaen et al., 2016), and groundwater and riparian inputs (Dick et al., 2015). Because these processes are challenging to quantify at the network scale, leveraging spatial autocorrelation to analyze patterns in labile constituents may offer improvements over models employing only aggregate watershed attributes (Peterson et al., 2006).

The spatial scale (resolution and extent) at which watershed features are quantified, and instream sampling distance and frequency also influence interpretations of ecological or biogeochemical processes shaping streamwater constituents (Loreau et al., 2013; McGuire et al., 2014; Wiens, 1989). Landscape *composition* provides information on the relative or absolute amounts of watershed attributes, while landscape *configuration* provides information on where those features are located relative to one another or relative to a point of interest such as a sampling location in the river channel. Dendritic river networks have a nested hierarchical spatial arrangement, and linkages between landscape composition, configuration, and instream conditions are scale dependent (Hunsaker & Levine, 1995). For example, geologic units shaping stream chemistry may span hundreds or thousands of km and would be considered "broad-scale" features that extend for large swaths of a watershed. However, geologic faults spanning several km can create finer-scale chemical heterogeneity between geologic units (Brennan et al., 2016). Similarly, topography can be quantified at broad scales (e.g., 100–1,000 km) via total watershed relief, or at finer scales (e.g., 10–100 m) using a metric like channel slope or local relief. Land cover can be quantified at fine scales (e.g., 30–50 m pixels) or aggregated for an entire watershed (100–1,000 km scale). Understanding how landscape features across a watershed influence instream biogeochemistry throughout river networks thus necessitates quantifying watershed conditions across a range of spatial scales.

Watershed attributes are often coarsely quantified at the aggregate watershed scale in terms of watershed composition (e.g., % cover), but few studies have evaluated the configuration (e.g., spatial location and extent) of watershed attributes governing streamwater chemistry in river networks (but

see Abbott et al., 2018; Shogren et al., 2019). Gergel et al. (1999) showed the importance of total watershed wetlands versus riparian wetland cover in determining instream DOC, and more recent work found that headwater bedrock outcrops may be substantial sources of calcium, magnesium, and silica minerals (Ingri et al., 2005) to downstream sites. Some work has shown that carbon and nutrient concentrations are best explained using whole watershed characteristics (Andersson & Nyberg, 2008; Varanka & Hjort, 2016). However, in boreal stream networks the majority (90%) of hydrologic connectivity between catchment features and stream channels occurs in low-order headwaters (Ledesma et al., 2018) that are often characterized by rich organic soils, but to our knowledge no study has examined the effects of headwater versus higher-order catchment features on stream biogeochemistry across an entire boreal river network.

Recently developed SSN models (Peterson & Hoef, 2010; Ver Hoef & Peterson, 2010) leverage spatial correlation among observations and partition instream variance among watershed features and downstream mixing and transport. This modeling approach provides a framework for studying the balance of watershed versus instream factors shaping streamwater constituents. Here we use SSNs to examine spatial patterns in constituents ranging from what we expect to be highly labile (NO_3^- and PO_4^{3-}) to highly conservative (Sr^{2+} and Ca^{2+}) and hypothesize that DOC spatial patterning is less patchy than nutrients and more patchy than conservative tracers due to limited instream processing along the network. We quantify watershed effects on streamwater constituent concentrations across multiple spatial extents according to stream order, while simultaneously accounting for spatial correlation in observations. In doing so, we identify the network position at which watershed features shape streamwater constituents and quantify the relative importance of watershed and instream effects.

2. Study Area

2.1. Watershed Overview

We conducted this study in the Kuskokwim River, a large (124,000 km^2) free-flowing, boreal river basin in western Alaska. The study region includes 54,000 km of channel length (second order and larger, Figure 1), with sample sites spanning second- to eighth-order streams. The Kuskokwim River is the largest free-flowing river in the United States and spans from headwaters in the Kuskokwim Mountains and glacially influenced tributaries of the Alaska Range (3,550 m) to its outlet in Kuskokwim Bay on the Bering Sea (0 m), with a mean discharge of 1,897 $m^3\ s^{-1}$ (U.S. Geological Survey, 2018).

2.2. Watershed Morphology

The Kuskokwim watershed is overlain by high elevation barren mountain ranges and broad boreal lowlands, rolling hills, and wetlands (Figure 1a). Basin geology reflects the progressive western growth of Alaska along the ancestral North American continental margin from the Precambrian to the early Cenozoic (Colpron et al., 2007). The geologic evolution of the watershed results in a strong east-west gradient in Sr isotopic signatures and Ca^{2+} and Sr^{2+} weathering patterns across the Kuskokwim basin (Brennan et al., 2014). Several major tributaries draining the Alaska Range carry high silt loads from glacial headwaters to the mainstem. Low-lying regions are predominantly overlain by Quaternary surficial deposits of glacial, alluvial, colluvial, and eolian origin and thick layers of organic material associated with peatlands and permafrost (Fernald, 1960). Braided alluvial channels span much of the piedmont, with meandering river floodplains in the lowlands.

2.3. Watershed Land Cover

Land cover within the Kuskokwim maps closely to the geomorphic template, comprising barren rock, snow, and glaciers in mountainous regions, mixed shrub and dwarf shrub in subalpine areas, wet and dry-type tundra, and mixed deciduous-evergreen forest in riparian corridors and lowlands below 600 m elevation (Fernald, 1960; U.S. Geological Survey, 2016). Wetlands dominate the low-lying western portion of the watershed at the Yukon-Kuskokwim delta and the low-relief interior between the Kuskokwim Mountains and Alaska Range to the north and east (U.S. Geological Survey, 2016). Modern peat soils are widespread in these bogs and adjacent lowlands, underlying muskeg vegetation, and variable soil types are mapped in higher relief areas (Fernald, 1960; Rieger et al., 1979). Discontinuous, sporadic, and isolated permafrost occur throughout the watershed at active layer depths of 0.5–2 m, with continuous permafrost in the upper reaches of the Tonzona River and Swift Fork (Fernald, 1960; Jorgenson et al., 2008).

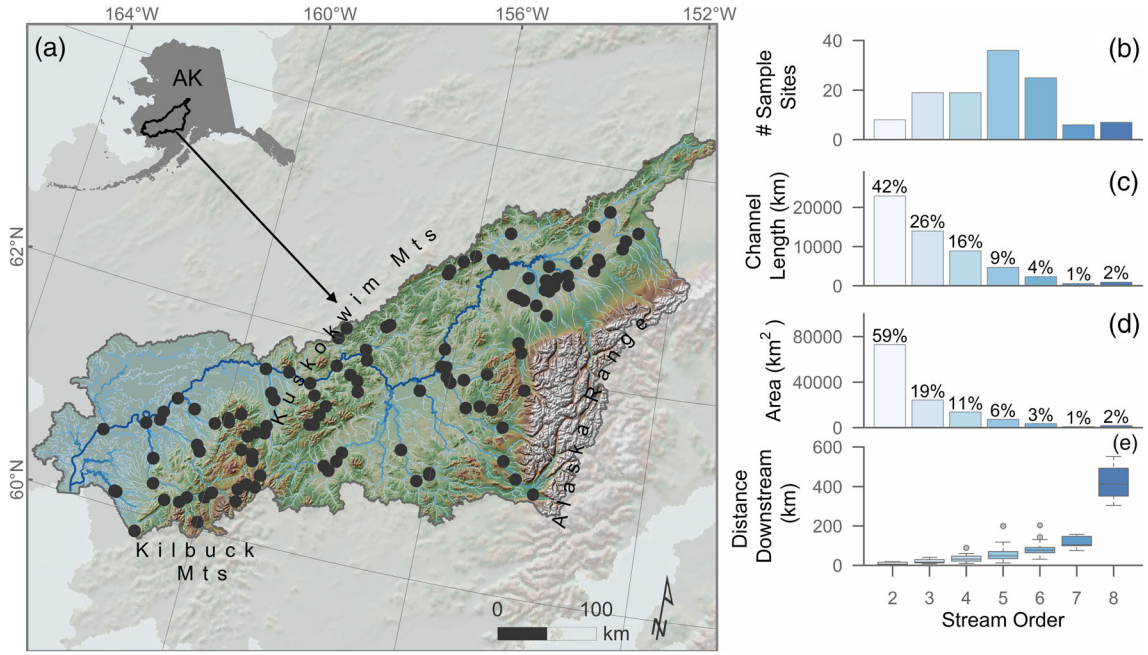

Figure 1. Map of the Kuskokwim River watershed study area and sampling locations (a) and sample counts by stream order (b). Total watershed channel length (c) and area (d) within each stream order and average downstream distance traveled from headwaters to each sample site based on sample site stream order (e).

2.4. Watershed Climate

Climate generally varies with elevation and latitude in the Kuskokwim. Modeled mean annual precipitation ranges from 36 cm in the lowlands to 296 cm in the Alaska Range and Kilbuck Mountains (Scenarios Network for Alaska and Arctic Planning (SNAP), 2017). High-altitude areas receive greater precipitation in the form of snow during the winter months, and summer rainfall from late July through August spans much of the watershed. As such, the hydrograph in the lower Kuskokwim peaks with snowmelt in late spring, followed by a smaller secondary peak in August (Figure S1 in the supporting information; U.S. Geological Survey, 2018). Mean summer temperatures in the watershed are lowest in the mountains (−1.9°C) and generally increase with latitude in the lowlands, with the highest mean summer temperatures (15.9°C) in the North Fork Kuskokwim (Scenarios Network for Alaska and Arctic Planning (SNAP), 2017).

3. Methods

3.1. Sample Collection

Water samples were collected in July and August of 2017 at 120 sites distributed across second- to eighth-order streams in the Kuskokwim watershed to maximize coverage of major land covers and stream orders (Figure 1b). Because first-order streams would have nearly doubled the number of channel segments in our study, first-order streams were omitted due to logistical constraints during sampling and to reduce computation times, but we acknowledge this limitation in our sampling design. Ninety of 120 sites were sampled in the span of 2 weeks in late July to early August, with the remaining sites along the mainstem and lower tributaries sampled by boat in mid-July and mid-August (Figure S1). Mainstem Kuskokwim discharge was generally increasing over the course of sampling but varied from 1,608–1,679 $m^3\ s^{-1}$ during our primary sampling effort ($n = 90$, Figure S1). At each sample site water was collected from the channel thalweg or at the maximum wadable depth, facing upstream of the collector after allowing channel bed disturbance to settle-out or mobilize downstream.

Samples for DOC and nutrients (NO_3^-, NO_2^-, and PO_4^{3-}) were syringe filtered through a 0.45 μm surfactant-free cellulose acetate (SFCA) filter after rinsing the syringe three times with sample water. DOC samples were filtered into 40 ml carbon-clean glass vials, and nutrient samples were filtered into acid-cleaned high-density polyethylene (HDPE) bottles. DOC and nutrient samples were stored in dark

and cold conditions then frozen at the end of each sample day and shipped frozen to the analytical lab every three to five sampling days throughout the sampling period. Water samples for trace elements (Ca^{2+} and Sr^{2+}) and Sr isotope analysis were collected into acid-cleaned, low-density polyethylene (LDPE) bottles after three rinses with sample water and filtered through a polyethylene Luer-lock syringe filter (0.45 μm polypropylene membrane) into acid-washed 125 ml LDPE narrow-mouth bottles within 48 hr of collection (Brennan et al., 2014). All trace element samples were stored in dark and cold conditions until analysis. To evaluate consistency in field collection methods, field triplicates were collected at five of the sample sites. Field-related contamination was evaluated through collection of five blank samples using the same methods described above for samples, but with NANOpure de-ionized water (Type I, 18.0 MΩ).

4. Sample Analyses

4.1. DOC Analyses

DOC samples were analyzed at the University of Washington Marine Chemistry Laboratory (UWMCL) following Environmental Protection Agency (EPA) standard method 5,310 B-00 (www.standardmethods.org) and protocols detailed in UNESCO (IOC, 1994) on a Shimadzu TOC-Vcsh carbon analyzer (Shimadzu Scientific Instruments, Kyoto, Japan), using the high-temperature catalytic oxidation method and measured on a non-dispersive infrared detector. Water samples were acidified with 6N HCl and sparged prior to analysis. The limit of quantitation (LoQ) for these analyses was estimated at 20.0 μg L^{-1}. Blanks were all below the LoQ and analytical precision (2SE [standard error]) between triplicate samples was ±30.0 μg L^{-1}.

4.2. Nutrient Analyses

Nutrient samples were analyzed at UWMCL following UNESCO (IOC, 1994) and EPA standard methods 353.4-2-1997 (NO_3^-), 353.4-2-1997 (NO_2^-), and 365.5-1.4-1997 (PO_4^{3-}, www.epa.gov/nerl) on a SEAL AA3 (SEAL Analytical, Norderstedt, Germany). Standards and blanks were analyzed at the start and end of all sample batches. LoQs were 4.0, 0.2, and 0.4 μg L^{-1} for NO_3-N, NO_2-N, and PO_4-P, respectively. All blanks ($n = 8$) were below LoQs, and analytical precision between triplicate samples was ±0.25, 0.02, and 0.09 μg L^{-1} for NO_3^-, NO_2^-, and PO_4^{3-}, respectively. Measurements are reported as NO_3-N, NO_2-N, and PO_4-P in μg L^{-1}. Analytical zeroes and samples below LoQs were assigned a fixed value of one-half the LoQ for all statistical analyses (2.1 μg L^{-1} for $NO_2^- + NO_3^-$ and 0.2 μg L^{-1} for PO_4^{3-}, e.g., Likens & Buso, 2006; Shogren et al., 2019).

4.3. $^{87}Sr/^{86}Sr$ Analyses

$^{87}Sr/^{86}Sr$ samples were acidified using 2 ml ultrapure concentrated HNO_3 (BDH Aristar Ultra) at the University of Utah Department of Geology and Geophysics inductively coupled plasma mass spectrometry (ICPMS) laboratory within 2 weeks of sample collection. $^{87}Sr/^{86}Sr$ ratios were determined using multi-collector (MC) ICPMS (Thermo Scientific, High Resolution NEPTUNE, Bremen, Germany). The $^{87}Sr/^{86}Sr$ ratio of the standard reference material (SRM) 987 (NIST; www.nist.gov) was determined to be 0.71028 ± 0.00001 (2σSE). The $^{87}Sr/^{86}Sr$ ratios were corrected for mass bias using an exponential law, normalizing to $^{86}Sr/^{88}Sr = 0.11940$ (Steiger & Jager, 1977). Isobaric interferences were corrected by simultaneous monitoring of ^{85}Rb and ^{83}Kr using corresponding assumed invariant ratios $^{87}Rb/^{85}Rb = 0.38571$ and $^{86}Kr/^{83}Kr = 1.50252$ (Steiger & Jager, 1977). Analytical precision (2SE) of field triplicates was determined to be ±0.00002, and analytical precision of all water samples ranged from ±0.000004–0.00002.

4.4. Elemental Analyses

Ca^{2+} and Sr^{2+} samples were acidified using 2 ml ultrapure concentrated HNO_3 (BDH Aristar Ultra) at the University of Utah ICPMS laboratory within 2 weeks of sample collection. Analyses were conducted using an Agilent 7500ce ICPMS (Agilent Technologies, Santa Clara, CA, USA). Samples were diluted 4:1 with 2.4% ultrapure HNO_3 (BDH Aristar Ultra) and Indium (25 ng ml^{-1}) was added as an internal standard. $[Sr^{2+}]$ and $[Ca^{2+}]$ were determined using a six-point calibration curve. SRM 1343e (NIST) was analyzed after every 30 samples ($n = 4$) and $[Sr^{2+}]$ and $[Ca^{2+}]$ in SRM1343e were within 3.2% and 3.6% of respective reference values. Precision of field triplicates was ±0.88 μg Sr^{2+} L^{-1} and ±170 μg Ca^{2+} L^{-1} and blanks were below LoQs (maximum LoQs of all runs were 0.60 μg Sr^{2+} L^{-1} and 1,030 μg Ca^{2+} L^{-1}, respectively).

5. Statistical Analysis

We used a statistical modeling approach that includes watershed attributes and accounts for spatial autocorrelation among sampling sites throughout the Kuskokwim based on flow connectivity, flow magnitude, and flow direction (Ver Hoef & Peterson, 2010) to understand how biogeochemical constituents were transported throughout the river network. This approach allowed us to partition variance in streamwater constituents between watershed and instream factors.

We first used empirical semivariograms to identify spatial autocorrelation among sample sites and evaluate the range at which watershed attributes might be important (McGuire et al., 2014). We then fit SSN models for each streamwater constituent throughout the network using watershed attributes derived at 14 different extents based on stream order (Figure 2). Model performance for each constituent was assessed across these spatial extents to identify the network position or extent where watershed attributes most strongly influence streamwater constituents. The relative importance of instream versus watershed effects was then compared across streamwater constituents ranging from labile (e.g., PO_4^{3-}) to biogeochemically conservative (e.g., Sr^{2+}).

5.1. Empirical Semivariograms

Empirical semivariograms show the strength of spatial correlation between sites across a range of distances (Olea, 1994), and observed patterns can yield insights into the spatial structure of ecological or biogeochemical processes governing streamwater constituents (McGuire et al., 2014). Distance in a semivariogram is traditionally measured as the Euclidean, or straight line, distance between two sample points (Matheron, 1963). For data on stream networks, and especially for streamwater constituents where downstream transport and processing are important (Closs et al., 2004), hydrologic distance between sites sharing flow (flow-connected) is often a more meaningful spatial dimension for assessing spatial structure (Cressie et al., 2006; Ganio et al., 2005; Peterson et al., 2006). We compared semivariance in both Euclidian and flow-connected spatial dimensions to examine watershed and instream effects on spatial structuring in streamwater constituents using

$$\gamma(h) = \frac{1}{2|N(h)|} \sum_{N(h)} \left(z_i - z_j\right)^2, \quad (1)$$

where γ is semivariance, $N(h)$ is the set of all pairwise distances $i - j = h$, $|N(h)|$ is the number of distinct pairs in $N(h)$, and z_i and z_j are data values at spatial locations i and j, respectively (Matheron, 1963). We used a maximum separation distance of 1,200 km, 40 lag bins, and a minimum of 15-point pairs per lag bin in semivariance computations. Semivariograms for stream constituents were assessed visually in terms of general trends in both Euclidian and flow-connected spatial dimensions, range (distance of asymptote or peak in semivariance), nugget (variance at finest spatial scale), and nested spatial structures as denoted by inflection points in the data (McGuire et al., 2014; Rossi et al., 1992).

5.2. SSN Models

We used SSNs to analyze streamwater constituent concentrations that differ in their expected biological lability (DOC, $NO_3^- + NO_2^-$, PO_4^{3-}, Ca^{2+}, and Sr^{2+}) and $^{87}Sr/^{86}Sr$ ratios for all sites sampled ($n = 120$). These models are described in detail elsewhere (Peterson & Hoef, 2010; Ver Hoef et al., 2006; Ver Hoef & Peterson, 2010). In brief, SSNs explicitly account for complex relationships within a stream network and provide flexible covariance structures for stream data and leverage spatial autocorrelation among sample sites to improve model performance (Peterson et al., 2006, 2007). Covariance is determined via both hydrologic and Euclidean distance. Spatial relationships among sites are incorporated into covariance matrices via moving average spatial autocorrelation functions (Ver Hoef & Peterson, 2010).

We used a mixed-effects modeling framework in which the observed variance in a constituent across the river network (e.g., [DOC]) is explained by a set of watershed attributes modeled as fixed effects (e.g., % bog cover and basin slope) and spatial covariance matrices as random effects. The general form of the spatial linear mixed model is as follows:

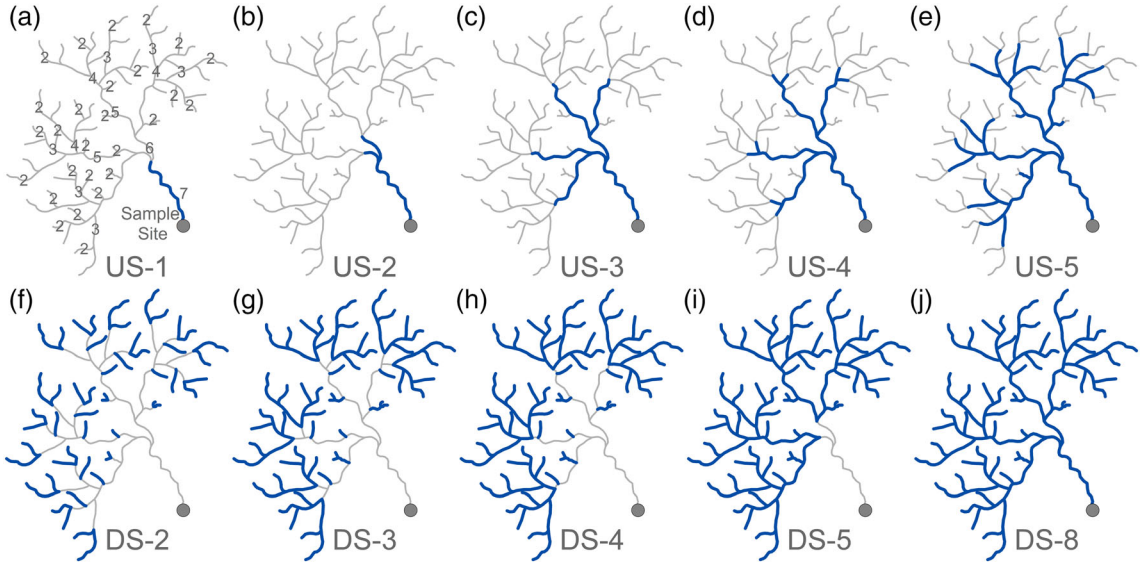

Figure 2. Diagrams of spatial scaling approach for deriving watershed attributes by stream order moving upstream (a–e) and downstream (f–j). Upstream (US-) scaling begins with local watershed attributes at a sample site and iterates upstream by one stream order for each scale. Downstream (DS-) scaling begins with second-order streams and iterates downstream by one stream order for each scale.

$$y = X\beta + z_H + z_E + \epsilon, \tag{2}$$

where y is the vector of a response variable (e.g., [DOC]), X is a matrix of covariates (e.g., watershed attributes such as % bog cover), β is a vector of parameters for each covariate in X, z_H and z_E are vectors of random variables with hydrologic (flow-connected) and Euclidean correlation structures, respectively, and ϵ is a vector of independent random errors.

Autocovariance functions for flow-connected relationships within the SSNs require a spatial weight or segment proportional influence (SPI) to inform how the moving average function behaves at stream confluences (Ver Hoef et al., 2006). We derived SPI based on watershed area and precipitation amount as a proxy for stream flow (e.g., Peterson et al., 2007). To estimate stream flow proportional to watershed area, we used gridded decadal mean annual precipitation (Table S1) throughout the entire Kuskokwim basin and accumulated all grid cells upstream of each stream segment using the Spatial Toolbox for the Analysis of River Systems (STARS) toolbox in ArcGIS (Peterson & Hoef, 2014). Flow accumulation and a synthetic channel network for input to the SSNs were derived from a digital elevation model (DEM) extracted from the U.S. Geological Survey (USGS, 2017) National Elevation Dataset.

5.2.1. Watershed Attributes

Watershed attributes were compiled using the STARS toolbox and publicly available geospatial data sets (Table S1) (Peterson & Hoef, 2014). Resolution of watershed attributes ranged from 30 m raster data sets (e.g., land cover and slope) to broader scale (100–1,000 km) vector-based data (geologic units, and soil classes), and watershed areas for sample sites ranged from 0.2–116,000 km^2 (Table S1 in the supporting information [SI]). To compare covariate effect sizes in final models, all watershed attribute covariates were standardized to a mean of 0 and standard deviation of 1. Correlations between watershed attributes and streamwater constituents were evaluated and ranked in exploratory analyses. A set of a priori candidate models was developed for each streamwater constituent with watershed covariates selected based on predictors for other study systems and factors which we hypothesized to affect streamwater constituents. Multi-collinearity was assessed using variance inflation factors (VIF), with collinear covariates removed from candidate models. A complete list of watershed attributes, value ranges, data resolutions and sources is in Table S1.

For all constituents, modeled mean annual precipitation, watershed slope, and watershed relief were included in candidate models as these watershed features are expected to affect the movement of water and solutes from uplands to the stream channel (Lintern et al., 2018; Smits et al., 2017). We expected

positive correlations between DOC and features related to the accumulation of soil organic matter, such as low basin relief, peat bogs, and wetland areas (e.g., Agren et al., 2014; Gergel et al., 1999; Laudon et al., 2011; Mulholland, 1997; Varanka et al., 2015). Because no complete wetland inventory is available for the entire Kuskokwim watershed, we used separate geospatial data sets for peat bogs, open water wetlands, marshes, and spruce forest swamps (Table S1).

NO_3^- and NO_2^- (hereafter referred to as "NO_3^-") were pooled for each site and modeled together. Candidate models for NO_3^- included alder (*Alnus* spp.) plant cover, which has been shown to influence NO_3^- concentrations in Alaska streams (Callahan et al., 2017; Hiatt et al., 2017; Shaftel et al., 2012). NO_3^- is also negatively correlated with DOC in some Alaska watersheds (Harms et al., 2016), with steeper basins having higher NO_3^- and lower DOC (Rodriguez-Cardona et al., 2016; Walker et al., 2012). This is likely related to both shorter residence times limiting N transformations in steeper basins and organic matter accumulation and soil saturation fueling microbial denitrification and N-limitation in lower relief basins. DOC measurements were included in candidate models for NO_3^- and PO_4^{3-} to evaluate this relationship in the Kuskokwim.

Ca^{2+}, Sr^{2+}, and PO_4^{3-} are generally influenced by rock weathering in high relief areas where bedrock exposures correspond with mechanical weathering and higher precipitation, and $^{87}Sr/^{86}Sr$ are strongly correlated with surface geology and precipitation in much of western Alaska (Bataille et al., 2014; Brennan et al., 2015; Brennan et al., 2019). Surface geology was simplified into 12 major groups based on lithology type and age from the Global Lithological Map database (Hartmann & Moosdorf, 2012). A priori candidate models for PO_4^{3-} included apatite-bearing geology types and candidate models for Ca^{2+} and Sr^{2+} included mafic and calcareous lithologies, predominantly within mixed sedimentary classes.

5.2.2. Spatial Scaling

Watershed attributes upstream of each sample site were quantified at 14 different nested spatial extents (Figure 2). We derived watershed attributes with increasing upstream extents by including only watershed attributes for the local catchment area draining to the sample site between stream confluences and then iterating upstream to include contributing areas based on the sample site's stream order, the site's stream order and drainages for stream order −1, stream order −2, and so forth until the entire upstream drainage was accounted for (Figures 2a–2e). We also derived watershed attributes in a downstream direction by including only second-order stream basins, second- to third-order basins, second- to fourth order, second to fifth order, second to sixth order, second to seventh order, second to eighth order, and all stream orders (Figures 2f–2j). In doing so, we evaluate the effect of small-, low-order stream catchments on downstream biogeochemical conditions. By evaluating the effect of watershed attributes across both upstream and downstream spatial extents, we quantified the effect of local and distant watershed features on streamwater constituents at each sample point in the Kuskokwim network.

5.2.3. Model Selection

SSN models were initially fit with single watershed attributes using the SSN package in R (Ver Hoef & Peterson, 2010) using maximum-likelihood parameter estimation. For these model fits, all runs used the same random effect structure with exponential tail-up (flow-connected) and Euclidean spatial autocovariance components (Ver Hoef et al., 2014). Univariate models were compared using root-mean-square prediction error (RMSPE) derived from leave-one-out cross validation (LOOCV) predictions and a spatial corrected Akaike information criterion (AIC_c) (Hoeting et al., 2006), which is similar to standard AIC but penalizes models based on the number of parameters used to estimate the spatial autocovariance structure:

$$AIC_c = -2\ell_{profile} + 2n\frac{p+k+1}{n-p-k-2} \quad (3)$$

where ℓ_{profile} is the profile log-likelihood function (Cressie, 1993), n is the sample size, $p-1$ is the number of covariates, and k is the number of autocorrelation parameters.

Additional watershed attributes were then combined iteratively with the best-performing univariate models in a stepwise fashion and again selected using RMSPE and AIC_c. The best combination of watershed attributes for each streamwater constituent was then used to parameterize the spatial autocovariance structures using restricted maximum likelihood estimation. We expected watershed attributes (e.g., % bog) to capture the Euclidean spatial structure in our data and for instream processing and transport to comprise the

flow-connected dimension. As such, initial models were fit using only watershed attributes and flow-connected autocovariance. We then computed empirical semivariance for residuals to evaluate any remaining spatial structure in the Euclidean and flow-unconnected dimensions. For constituents with spatially autocorrelated residuals, we then tested different combinations of spatial autocorrelation functions in the flow-connected and Euclidean dimensions (e.g., exponential, Gaussian, and linear with sill) (Ver Hoef & Peterson, 2010) and again used AIC_c to select the spatial autocovariance structure for each streamwater constituent. Residual semivariance was then computed to check for remaining spatial autocorrelation, normality, and homoscedasticity. For comparison, we also parameterized models with only watershed attributes using non-spatial multiple linear regression, and SSN models with only Euclidian and only flow-connected autocovariance (Table S4).

5.2.4. Streamwater Constituent Comparison

The flexible covariance structures in SSN models are well-suited for evaluating the relative effects of instream processing and transport (flow-connected) and watershed attributes by examining variance composition (Ver Hoef et al., 2014; Ver Hoef & Peterson, 2010), which is partitioned among the various autocovariance structures (e.g., Euclidian and flow-connected) and watershed attributes. Variance composition was determined for each constituent at each spatial extent and compared across constituents and across spatial extents. In doing so, we compared the behavior of the constituents (e.g., conservative Sr vs. biologically reactive NO_3^-) and identified the spatial extents at which watershed attributes explained the greatest variance.

6. Results

6.1. Spatial Structuring in Streamwater Constituents

All streamwater constituents exhibited distinct spatial patterns across the Kuskokwim watershed, but the scales of these patterns varied by constituent and by spatial distance metric (e.g., stream order and Euclidian vs. hydrologic, Figure 3). All streamwater constituents generally trended toward watershed average values with distance downstream (dashed horizontal line in Figures 3a–3f). Variation in constituent concentrations was generally highest within the first 100–150 km of the stream network (Figures 3a–3f), corresponding with second- to fifth-order channels (Figures 1e and 3g–3l). Mean $[PO_4^{3-}]$ and [DOC] were lowest in second-order streams and generally increased with stream order. $[Sr^{2+}]$ and $[Ca^{2+}]$ decreased from second- to sixth-order streams, followed by increases in seventh- and eighth-order streams (Figures 3g–3l). Mean values for $[NO_3^-]$ and $^{87}Sr/^{86}Sr$ showed no major differences among stream orders; however, $[NO_3^-]$ variance was lowest in seventh- and eighth-order streams and mean $^{87}Sr/^{86}Sr$ was highest and $^{87}Sr/^{86}Sr$ variance was lowest in second-order streams (Figure 3l).

Semivariograms revealed distinct contrasts in the spatial structuring of different chemical constituents across the watershed (Figures 3m–3r). Increases in semivariance with distance indicate positive spatial autocorrelation (nearby sites are more similar), and inflection points in semivariance may indicate spatial structure at multiple spatial scales (e.g., McGuire et al., 2014). Semivariance in [DOC] and nutrients had a larger nugget (semivariance at shortest lag distance) than conservative tracers, indicating greater variability among samples at the finest sampling distance. $[PO_4^{3-}]$ and $[NO_3^-]$ were spatially autocorrelated in the flow-connected dimension to a range of roughly 200 km, with some evidence of additional flow-connected spatial structure exhibited by inflection points at 200 and 500 km for $[PO_4^{3-}]$ (Figures 3m and 3n). Both [DOC] and $[PO_4^{3-}]$ exhibited Euclidian spatial autocorrelation at multiple scales, with inflection points at roughly 200 and 400 km (Figures 3m and 3o). $[NO_3^-]$ Euclidian semivariance also had a range of roughly 200 km, with no clear signs of multiple scales in spatial patterning (Figure 3n).

Conservative constituents showed strong spatial autocorrelation in both Euclidian and flow-connected semivariance at broad distances spanning much of the sampling area (Figures 3p and 3r). Flow-connected semivariance for $[Sr^{2+}]$, $[Ca^{2+}]$, and $^{87}Sr/^{86}Sr$ increased up to 300 km, with declining semivariance for $^{87}Sr/^{86}Sr$ at distances beyond 300 km. Inflection points in flow-connected semivariance for both $[Ca^{2+}]$ and $[Sr^{2+}]$ occurred at 250 and 500 km. Euclidian semivariance increased to a range of approximately 350 km for $[Ca^{2+}]$ and 400 km for $[Sr^{2+}]$. Euclidian semivariance for $^{87}Sr/^{86}Sr$ increased beyond the range of our sample sites.

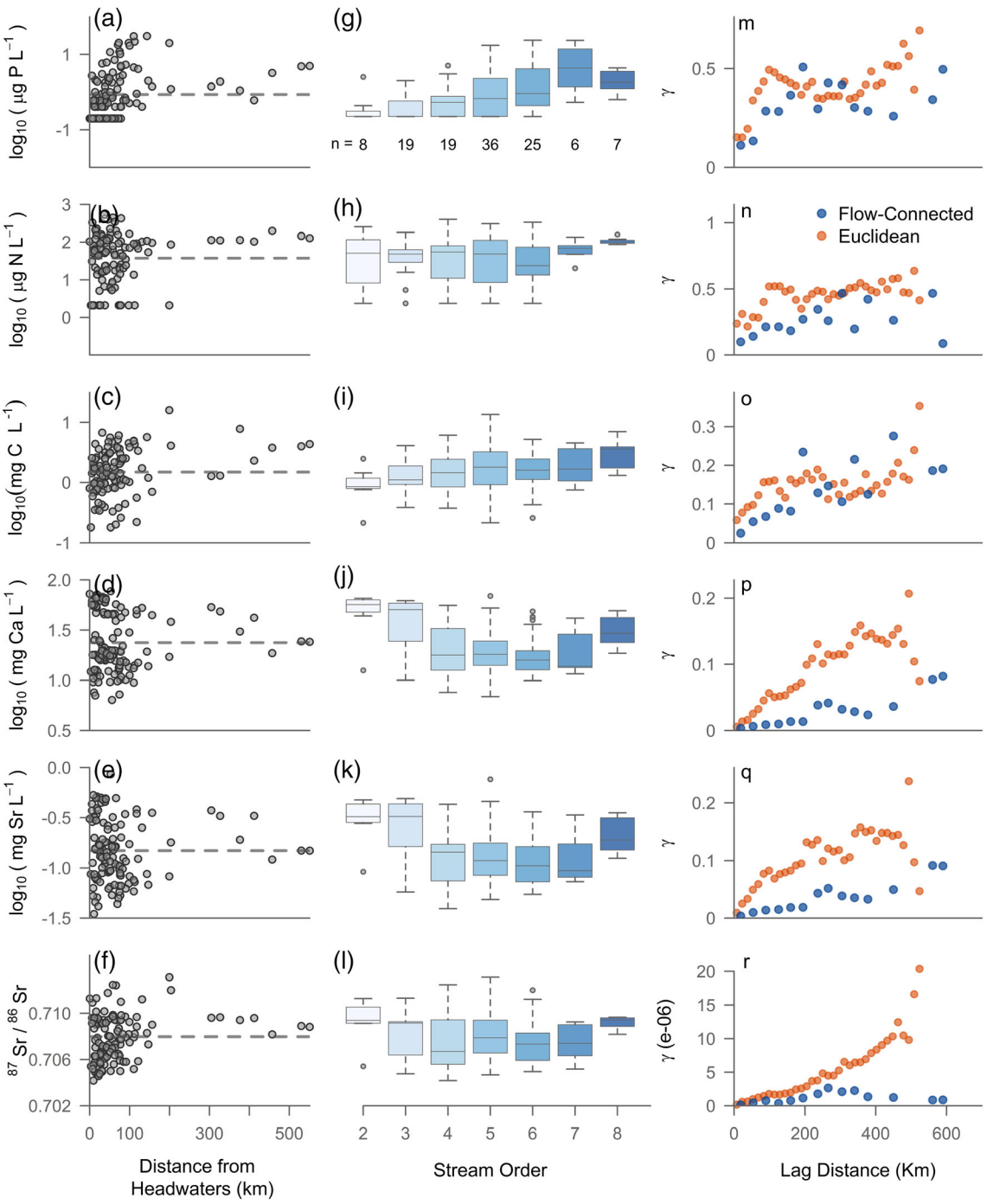

Figure 3. Streamwater constituent concentrations with average distance from headwaters for each sample site (a–f) and by stream order (g–l). Dashed horizontal lines in (a)–(f) are drawn at the mean value. Boxes in (g)–(l) include the interquartile range (IQR) and whiskers extend to 1.5 times the IQR from first and third quartiles. Empirical semivariograms (m–r) are plotted based on flow-connected (blue) and Euclidian distance (orange).

6.2. Watershed Covariates Governing Streamwater Constituents

Based on AIC_c, RMSPE, and LOOCV-R^2, the best SSN models for streamwater constituents in the Kuskokwim River included watershed attributes reflecting both broad (100–1,000 km) and fine (30–1,000 m) scale watershed attributes (Figures 4 and S2 and Table S2). For all constituents in our study, watershed attributes alone explained only 11–35% of chemical variation (Table S3) and could be grouped

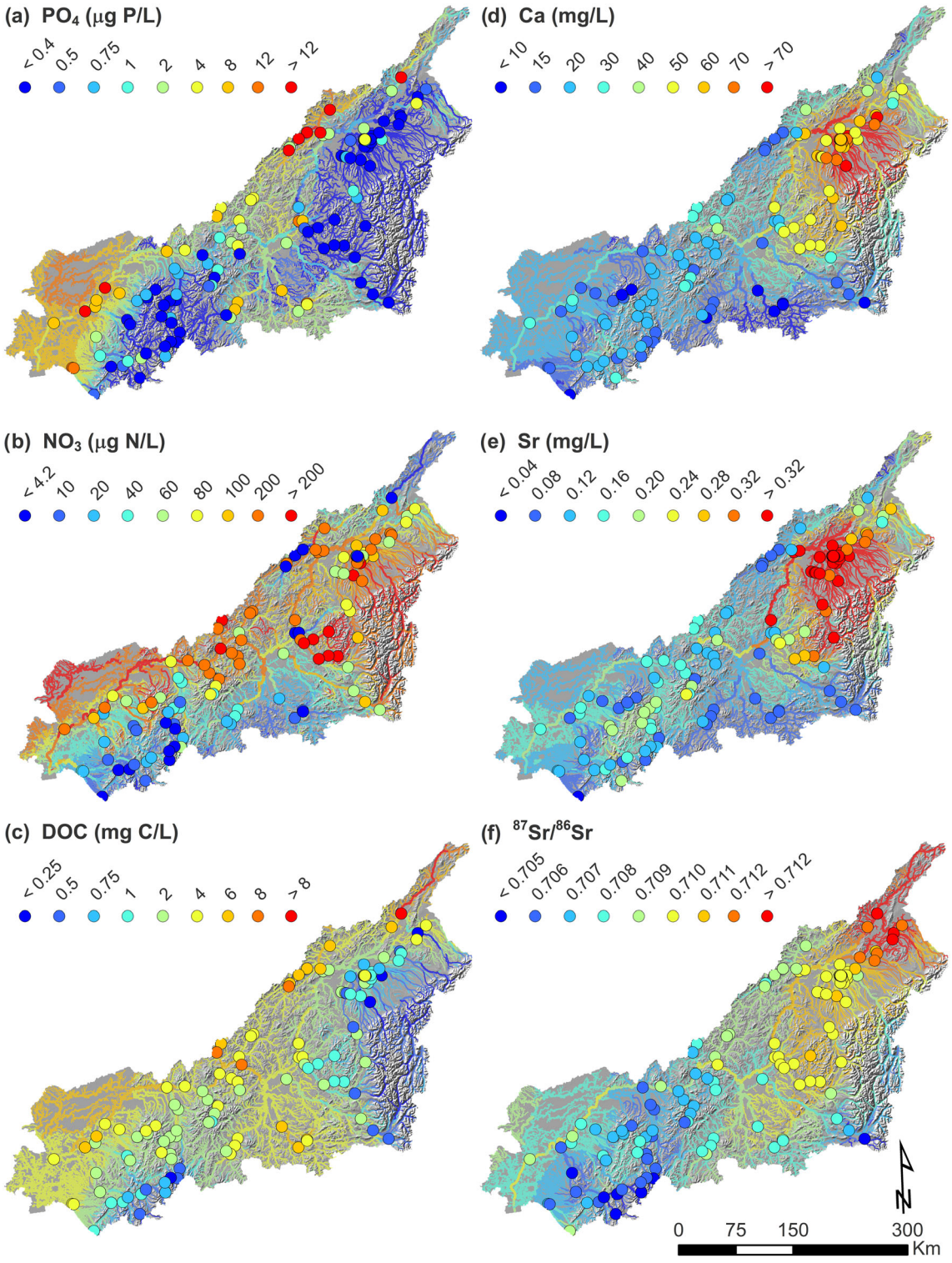

Figure 4. Watershed maps of streamwater constituent values at each sample point. Stream segments are colored based on predicted values from spatial stream network models for streamwater constituents for all second- to eighth-order channels in the Kuskokwim River. Model covariates and parameters are presented in Table S2.

into three primary drivers: (1) watershed relief, (2) land cover shaped by watershed morphology, and (3) the Farewell Terrane geologic unit. Sample site constituent measures and significant covariates for watershed attributes are mapped in Figure S2, with goodness of fit metrics in Table S2.

The best model for [PO_4^{3-}] included covariates for the watershed cover by the Farewell Terrane, sample site [DOC], and watershed area cover by sedimentary rock (Figure S2a). [PO_4^{3-}] was generally lower in the mountainous portions of the watershed (Figure 4a). NO_3^- spatial patterns were patchier across the watershed, with highest concentrations in streams draining the lower slopes of the Alaska Range and in the central Kuskokwim. [NO_3^-] was best modeled using covariates for watershed alder (*Alnus* spp.) plant cover, sample site [DOC], watershed latitude, and mean watershed elevation. [DOC] was highest in low-gradient portions of the Kuskokwim, with streams draining the Alaska Range and Kuskokwim/Kilbuck Mountains generally having lower DOC (Figure 4c). The best model for [DOC] included only mean watershed relief and watershed latitude (Table S2).

[Ca^{2+}] and [Sr^{2+}] in the Kuskokwim generally followed similar spatial patterns: high concentrations in portions of the Alaska Range coinciding with the Farewell Terrane and lower concentrations in the western watershed (Figures 4d and 4e). [Sr^{2+}] were also elevated in some portions of the Kilbuck mountains (Figure 4e). The best model for [Ca^{2+}] included watershed cover by the Farewell Terrane, acidic volcanic and plutonic rocks, intermediate volcanic and plutonic rocks, and mean watershed elevation. The best model for [Sr^{2+}] included these same watershed attributes, except for intermediate volcanic and plutonic rocks in place of acidic volcanics.

$^{87}Sr/^{86}Sr$ was highest in the northeastern portion of the Kuskokwim, with high values spanning the Farewell Terrane, and $^{87}Sr/^{86}Sr$ generally decreasing toward the western watershed (Figure 4f). The best model for $^{87}Sr/^{86}Sr$ included the Farewell Terrane, watershed relief, watershed extent covered by the last glacial maximum, intermediate volcanic and plutonic rocks, and siliciclastic sedimentary rock units in the Kilbuck and Kuskokwim mountains (Figure S2f).

6.3. Variance Composition Across Constituents and Spatial Scales

For most constituents in our study, models with watershed attributes derived at spatial extents emphasizing low-order headwater stream catchments performed the best, with watershed attributes and Euclidian spatial autocorrelation accounting for more of the overall variance for conservative constituents, compared to models for labile constituents (Figure 5). In general, watershed attributes for most constituents performed better as spatial extent increased in the upstream direction to include more of the headwaters and low-order streams (Figures 5a–5f). Moving in the downstream direction, models accounting for watershed attributes in second- to third-order streams generally performed as well or better than watershed-wide attributes (Figures 5g–5l).

Predictive power (LOOCV-R^2) generally increased from labile (PO_4^{3-}) to conservative ($^{87}Sr/^{86}Sr$) constituents, and labile nutrients and DOC had a larger nugget effect (Figure 5). The best models based on LOOCV-R^2, RMSPE, and AIC_c used watershed attributes derived at DS-3 for PO_4^{3-}, DOC, Ca^{2+}, and Sr^{2+}; at DS-2 for NO_3^-, and US-4 for $^{87}Sr/^{86}Sr$ (Table S2 and S3).

Watershed attributes accounted for roughly a third of variance in all constituents except for NO_3^-, with Euclidian spatial autocorrelation accounting for the majority of variance for all constituents except for PO_4^{3-}. Flow-connected spatial autocorrelation accounted for a lower proportion of variance than Euclidian and watershed effects across all constituents but was slightly higher for DOC and nutrients than for conservative tracers.

7. Discussion

7.1. Spatial Patterns in Streamwater Chemistry Throughout the River Network

Spatial patterning in streamwater chemical conditions across the Kuskokwim watershed revealed several differences in both watershed effects and instream transport behavior between the labile (PO_4^{3-} and NO_3^-) and conservative (bulk DOC, Ca^{2+}, Sr^{2+}, and $^{87}Sr/^{86}Sr$) constituents in our study. For all constituents we measured in the Kuskokwim, high chemical variation in the upper 100–150 km of stream channels highlights the importance of headwater and low-order catchment conditions in governing biogeochemical

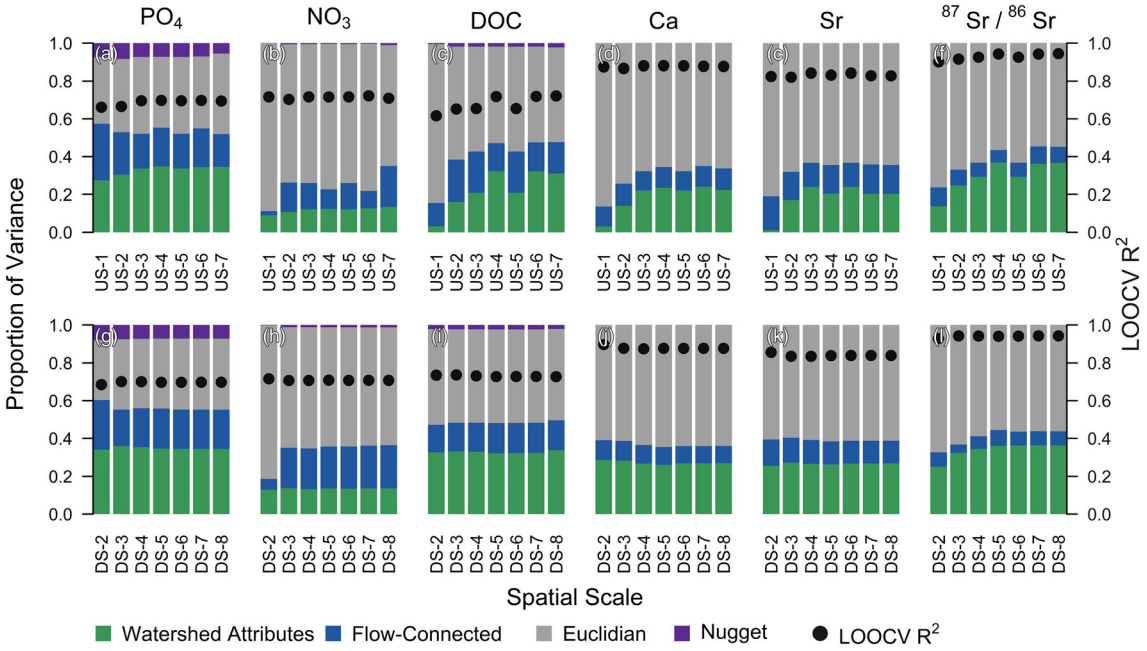

Figure 5. Variance composition and leave-one-out-cross-validation R^2 statistics (black dots) from spatial stream network models for all constituents across upstream (a–f) and downstream (g–l) spatial scales. Variance composition includes the proportion of overall variance explained by watershed effects (green bars), flow-connected spatial autocorrelation (blue bars), Euclidian spatial autocorrelation (gray bars), and the nugget or random error (purple bars).

heterogeneity across the river network. However, despite considerable spatial heterogeneity in smaller watersheds, all constituent concentrations in the Kuskokwim trended toward the watershed average with distance downstream. These trends toward watershed average values reflect flow-weighted contributions from a mixture of more variable, low-order streams.

These results are consistent with work in other rivers showing greater biogeochemical variation among smaller catchments and decreasing variation at broader scales (Abbott et al., 2018; Likens & Buso, 2006; Shogren et al., 2019; Temnerud et al., 2010, 2007). In large watersheds where many processes influence biogeochemical patterns, streamwater chemistry in larger streams tends to be homogenous (Likens & Buso, 2006). Previous work examining the watershed patch size at which variance collapse occurs found smaller extent patches (3–61 km^2) for labile constituents and larger extent patches (113–216 km^2) for conservative constituents (Abbott et al., 2018; Shogren et al., 2019), which correspond with second- to third-order watersheds in the Kuskokwim (47–208 km^2). For labile nutrients like PO_4^{3-} and NO_3^-, this pattern of variance collapse is likely due to some combination of higher cumulative uptake with distance downstream and shorter residence times in larger channels (Ensign & Doyle, 2006; Marcé et al., 2018; Mulholland et al., 2009), in addition to the expected spatial averaging that occurs as small tributaries combine into larger streams. Variance collapse in [DOC] has been attributed to net gains of allochthonous instream organic matter inputs along the network (Shogren et al., 2019). Recent work in boreal headwaters suggests that terrestrial DOC inputs may be passively transported in first- to fourth-order channels (Kothawala et al., 2015), while labile terrestrial DOC from permafrost can be metabolized instream within several weeks (Textor et al., 2019). Slight increases in [DOC] along the Kuskokwim network suggest that bulk DOC is simply transported through the river network with little instream processing. However, without measures of DOC composition, any instream processing of labile fractions is unknown. For the conservative tracers in our study, variance collapse and a trend toward watershed average values appears to reflect accumulation, transport, and mixing of heterogeneous landscape signals along the network. The spatial patterning of bulk DOC is largely consistent with these patterns. Higher Ca^{2+} and Sr^{2+} concentrations and $^{87}Sr/^{86}Sr$ values in low-order streams are consistent with higher mechanical weathering and precipitation in the mountainous headwaters of the Kuskokwim (Brennan et al., 2014).

Semivariograms revealed multi-scale watershed and instream effects on spatial patterning of chemical constituents across the Kuskokwim (Figures 3m–3r). Stronger spatial autocorrelation for the conservative tracers versus labile nutrients in our data set is consistent with instream cycling of biologically reactive constituents and conservative transport of Ca^{2+}, Sr^{2+}, and ^{87}Sr:^{86}Sr. The range of spatial autocorrelation was generally longer for conservative constituents, reflecting broad-scale watershed attributes and geomorphic gradients that influenced conservative constituents in the Kuskokwim. Sr^{2+} and $^{87}Sr/^{86}Sr$ in Alaska watersheds are shaped by broad-scale geologic features (Bataille et al., 2014; Brennan et al., 2016), and the range (300 km) of Euclidian spatial dependence for $[Ca^{2+}]$ and $[Sr^{2+}]$ coincides with the alkaline Farewell Terrane and the neighboring Kuskokwim Group. Inflection points in flow-connected semivariance for conservative constituents likely reflect major tributary inflows from these distinct geologies (Figures 4d–4f). $^{87}Sr/^{86}Sr$ Euclidian spatial dependence extended beyond the range of our sampling, despite strong correlation with the Farewell Terrane (Figure S2f). This pattern suggests a broader-scale process underlying Sr weathering not accounted for in our analyses.

Flow-connected spatial dependence in $[PO_4^{3-}]$ and [DOC] at broad scales (~600 km) likely also reflects mixing of streamwater influenced by gradients in latitude, relief, and geology, which were important attributes in best models for these constituents, whereas NO_3^- inputs appear patchier and unrelated to factors that vary smoothly from upstream to downstream. Inflection points in Euclidian semivariance in $[PO_4^{3-}]$ and [DOC] roughly coincide with the scale of the Farewell terrane and geomorphic gradients from high relief mountains to low-relief peat and bog environments in the Kuskokwim lowlands, which were included in our best models for $[PO_4^{3-}]$ and [DOC], respectively (Figure S2). Finer-scale (<200 km) spatial autocorrelation may reflect more local features such as wetlands or acidic peat soils that result in smaller patches of high [DOC] (McGuire et al., 2014).

7.2. Watershed Attributes Shaping Streamwater Constituents

Streamwater constituents in the Kuskokwim reflected watershed attributes occurring at multiple scales, such as geologic units or geomorphic features spanning several hundred kilometers and patches of alder cover spanning several hundred meters. Except for PO_4^{3-}, watershed relief or elevation were either directly included in the best SSN models for all constituents or indirectly included via land cover attributes or DOC, which are shaped by watershed geomorphology through effects on catchment hydrology, the accumulation of organic matter, and nutrient transformations. [DOC] is typically positively correlated with wetlands and peat bogs in boreal river systems (Agren et al., 2008; Laudon et al., 2011; Mulholland, 1997), and peat bogs in the Kuskokwim were strongly negatively correlated with watershed relief (Pearson correlation coefficient = −0.64, $p < 0.01$). Exclusion of wetlands or peat from the best SSN for [DOC] is due in part to collinearity between relief and wetland land cover types. Additionally, previous work has found watershed slope to be a better predictor of DOC flux than wetlands (Andersson & Nyberg, 2008). Furthermore, because our data only provide a snapshot of Kuskokwim biogeochemistry, seasonal hydrology may mask land cover effects on instream DOC to some extent (Laudon et al., 2011). For example, Buffam et al. (2007) showed reduced sub-catchment variation in DOC during spring runoff, when wetland signals were diluted and forest soils were flushed of organic matter. Sampling for our study was limited to the summer period when water levels are typically rising in the Kuskokwim (Figure S1); however, the inclusion of a random effect for sampling date had no improvements to models and in some cases increased parameter bias. While we did use a spatially explicit, precipitation-based weighting scheme for flow-connected models, our assumption of an equal runoff to basin area relationship across the watershed is likely overly simplistic but provides a first approximation for flow-weighting of tributaries. Furthermore, we did not capture seasonal effects of factors like temperature that influence primary productivity and active layer depth in soils, thereby shaping OM and nutrient retention (Hawkes et al., 2018; Winterdahl et al., 2016). One study in northern Alaska suggests that spatial patterning in DOC, NO_3^-, and PO_4^{3-} is consistent across seasons (Shogren et al., 2019). The positive effect of latitude on both [DOC] and $[NO_3^-]$ may be driven by watershed summer air temperature, which increases to the north and east in the Kuskokwim except for mountainous areas (Scenarios Network for Alaska and Arctic Planning (SNAP), 2017). Measuring streamwater constituents in the Kuskokwim across seasons would elucidate this relationship as well as seasonal hydrologic effects but was not captured in our work.

The inclusion of DOC as a predictor probably precluded watershed relief as a covariate in candidate models for PO_4^{3-}, given the strong influence of relief on [DOC] in the Kuskokwim and the positive relationship between [DOC] and [$PO4^{3-}$] in our data (Figure 4c). The negative relationship between [DOC] and [NO_3^-] in the Kuskokwim is likely linked to higher denitrification rates in drainages to DOC-rich streams. Low gradient watersheds have increased potential for saturated soils lending to both anaerobic conditions enhancing denitrification and longer residence times promoting N transformations (Lintern et al., 2018), and boreal streams draining peat/bog catchments generally have higher C:N (Aitkenhead & McDowell, 2000). Water saturated soils also prevent the establishment of N-fixing alder, one of the dominant sources of NO_3^- in western Alaska (Callahan et al., 2017; Devotta, 2017; Shaftel et al., 2012).

The positive relationship between relief and base cations and $^{87}Sr/^{86}Sr$ we observed in the Kuskokwim (Figure 4 and Table S2) has been shown for many rivers in western Alaska and is attributed to higher rates of physical erosion and exposed, reactive calcite in exposed rock material in steep basins (Brennan et al., 2014; Brennan et al., 2016). Portions of the high relief Alaska Range in the eastern Kuskokwim also coincide with the meta-sedimentary rocks and Paleozoic limestone in the Farewell Terrane, which yielded high concentrations of Ca^{2+} and Sr^{2+} in the eastern Kuskokwim basin (Figure S2) (Brennan et al., 2014).

Watershed morphology also shapes land cover types, which can modify or amplify watershed effects on instream biogeochemical patterning. In the Kuskokwim and in other Alaska watersheds (Callahan et al., 2017; Shaftel et al., 2012), [NO_3^-] was strongly positively correlated with alder (*Alnus* spp.) plant cover due to alder's N-fixing capacity. Previous work in southwest Alaska showed stronger relationships between alder and stream [NO_3^-] when alder cover exceeded 30% (Devotta, 2017). The upper range of alder cover in the Kuskokwim (at spatial scale DS-8) was 30.2%, with a median of 4.75%. [NO_3^-] measured by Devotta (2017) and by Shaftel et al. (2012) in Alaska subcatchments were roughly 3 times higher than the mean for the Kuskokwim (85.4 ± 9.26 [1 SE] $\mu g\ L^{-1}$). Despite lower overall [NO_3^-] and alder coverage, longer residence times and thus increased potential for denitrification in our study region, the strong relationship between alder and [NO_3^-] in the Kuskokwim highlights the importance of N-fixing alder in regulating stream nutrient availability in pristine boreal watersheds. The northward expansion of shrubs including alder is predicted to increase rapidly in boreal and subarctic regions under a warming climate (Pearson et al., 2013), and this expansion will likely alter nitrogen loading and nutrient stoichiometry.

7.3. Headwater Catchment Effects on Network-Wide Conditions

Headwater streams can account for up to 90% of channel length in boreal river networks (Bishop et al., 2008; Ledesma et al., 2018) and previous work shows that low-order streams can play a key role in terrestrial DOC processing (Bertuzzo et al., 2017), that headwaters regulate water and nutrient fluxes to larger rivers downstream (Alexander et al., 2007), and that biogeochemical heterogeneity is governed by conditions in small catchments (Abbott et al., 2018; Shogren et al., 2019; Zimmer et al., 2013). Low-order stream catchments in the Kuskokwim play an important role in regulating streamwater conditions across a large river network, and despite the routing of water over long (>500 km) distances, streamwater biogeochemistry in our study could be predicted as well or better by distant versus proximate watershed attributes. Low-order streams comprise the bulk of the Kuskokwim, and by very nature of dendritic spatial structure, all branched stream networks (Bishop et al., 2008). Ninety percent of our sample sites were on sixth-order or smaller streams (Figure 1b); thus, the bulk of Kuskokwim headwaters were included in watershed attributes derived at spatial extents larger than (to the right of- in Figure 2) US-4 in the upstream direction and DS-2 in the downstream direction. The increasing proportion of variance explained by watershed attributes in Figure 5 when moving upstream, with only minor or no changes when moving downstream also shows the effect of headwater attributes.

7.4. Watershed Versus Instream Effects on Streamwater Constituents

Two primary issues limit our ability to interpret instream versus watershed effects on streamwater biogeochemistry from SSN models: (1) separating Euclidian versus flow-connected variance in systems where Euclidian and flow-connected distances are often correlated is not possible, and as such, variance can be misattributed to one or the other; and (2) sampling at distance intervals greater than uptake length can lead to mischaracterization of instream processing. Despite these limitations, SSN models had markedly improved performance over non-spatial models, and accounting for the spatial configuration of the river

network in our analysis revealed spatial patterns that would not have emerged from non-spatial models or Euclidian metrics alone.

We expected flow-connected autocorrelation to account for a higher proportion of variance in conservative tracers and a lower proportion in labile constituents, but the opposite was true in the Kuskokwim. Flow-connected spatial autocorrelation accounted for only 4–18% of explained variance in [Ca^{2+}], [Sr^{2+}], and $^{87}Sr/^{86}Sr$, which was surprising given the passive transport of these solutes through the river network (Brennan et al., 2014; Brennan et al., 2016). The flexible nature of SSNs has interesting effects on variance composition; however, and when Euclidian autocorrelation was removed from SSN models, flow-connected covariance increased to account for up to 79% of explained variance (Table S4). Similarly, SSN models without flow-connected covariance apportioned up to 56% of variance to the Euclidian term. SSN models with both flow-connected and Euclidian covariance consistently had much lower proportion of variance apportioned to flow-connected covariance. This suggests that constituents in the Kuskokwim which were highly spatially autocorrelated within the stream channel were generally also highly correlated in Euclidian space due to the arrangement and/or scale of watershed attributes influencing streamwater constituents. Furthermore, the large proportion (up to 81% for NO_3^-) explained by Euclidian covariance in mixed SSN models indicates there were watershed attributes we excluded, and this pattern was true for all constituents. This may be due to the removal of collinear watershed attributes or a mismatch between the scale of mapped watershed attributes and effective patch size. Synoptic sampling of the watershed with finer-scale sampling distance would aid in differentiating between watershed and instream factors shaping streamwater constituents.

Based on semivariograms and variance composition, both DOC and PO_4^{3-} resembled conservative solutes (Ca^{2+}, Sr^{2+}, and $^{87}Sr/^{86}Sr$) more so than NO_3^-, which was generally patchier and had weak instream spatial structuring. It is difficult to interpret the degree of instream DOC processing for the Kuskokwim without measures of DOC composition. Previous studies provide ample evidence of instream DOC processing during transit along the river corridor (see reviews by Mineau et al., 2016, and Wohl et al., 2017), and labile DOC fractions are subject to rapid uptake and transformation during transit to river mouths in boreal streams (Weyhenmeyer et al., 2012; Weyhenmeyer & Conley, 2017). Labile material released from recently thawed permafrost is subject to more rapid uptake and decomposition than organic matter from seasonally thawed active soil layers (Textor et al., 2019; Wickland et al., 2018), and NO_3^- retention decreases as permafrost thaw depths increase (Harms & Jones, 2012). Under a warming climate, increases in labile DOC and NO_3^- inputs from permafrost regions to high-latitude rivers will likely modify the biogeochemical basis of aquatic food webs in boreal river networks.

8. Conclusions

Quantifying watershed effects on streamwater chemistry necessitates an accounting of the nested, hierarchical, spatial configuration of dendritic river networks and the downstream movement of water. SSNs provide a flexible, quantitative framework for studying stream biogeochemistry across entire river networks using a combination of field sampling and publicly available geospatial data. Low-order headwater streams generally account for the majority of watershed channel length and watershed area in dendritic river networks, and our study indicates that watershed attributes in these small catchments are key factors affecting stream biogeochemistry across a boreal river network. Understanding how watershed features shape spatial patterning for chemical drivers of aquatic food web productivity may aid the management of aquatic resources as watershed conditions change under a warming climate and growing developmental pressures.

Acknowledgments

We thank J. Baldock and D. Freundlich of the UW-Alaska Salmon Program, D. Fernandez, C. Anderson, and B. Munk at the University of Utah ICPMS Laboratory, Alaska Department of Fish and Game and U.S. Fish and Wildlife Service Yukon Delta National Wildlife Refuge staff, particularly L. Coggins, for assistance with field sampling, and A. Shapiro of Alaska Land Exploration. Funding for this research was provided by the Arctic-Yukon-Kuskokwim Sustainable Salmon Initiative and a National Science Foundation Graduate Research Fellowship (#DGE-1762114) to D. W. F.

Data Availability Statement

Data are available for non-commercial use (at https://doi.org/10.5281/zenodo.3828053). All geospatial data are publicly available, with references in Table S1.

References

Abbott, B. W., Gruau, G., Zarnetske, J. P., Moatar, F., Barbe, L., Thomas, Z., et al. (2018). Unexpected spatial stability of water chemistry in headwater stream networks. *Ecology Letters*, *21*(2), 296–308. https://doi.org/10.1111/ele.12897

Agren, A., Buffam, I., Berggren, M., Bishop, K., Jansson, M., & Laudon, H. (2008). Dissolved organic carbon characteristics in boreal streams in a forest-wetland gradient during the transition between winter and summer. *Journal of Geophysical Research*, *113*, G03031. https://doi.org/10.1029/2007JG000674

Agren, A. M., Buffam, I., Cooper, D. M., Tiwari, T., Evans, C. D., & Laudon, H. (2014). Can the heterogeneity in stream dissolved organic carbon be explained by contributing landscape elements? *Journal of Geophysical Research: Biogeosciences*, *11*, 1199–1213. https://doi.org/10.5194/bg-11-1199-2014

Aitkenhead, J. A., & McDowell, W. H. (2000). Soil C:N ratio as a predictor of annual riverine DOC flux at local and global scales. *Global Biogeochemical Cycles*, *14*(1), 127–138. https://doi.org/10.1029/1999GB900083

Alexander, R. B., Boyer, E. W., Smith, R. A., Schwarz, G. E., & Moore, R. B. (2007). The role of headwater streams in downstream water quality1. *JAWRA Journal of the American Water Resources Association*, *43*(1), 41–59. https://doi.org/10.1111/j.1752-1688.2007.00005.x

Andersson, J.-O., & Nyberg, L. (2008). Spatial variation of wetlands and flux of dissolved organic carbon in boreal headwater streams. *Hydrological Processes*, *22*(12), 1965–1975. https://doi.org/10.1002/hyp.6779

Bataille, C. P., Brennan, S. R., Hartmann, J., Moosdorf, N., Wooller, M. J., & Bowen, G. J. (2014). A geostatistical framework for predicting variations in strontium concentrations and isotope ratios in Alaskan rivers. *Chemical Geology*, *389*, 1–15. https://doi.org/10.1016/j.chemgeo.2014.08.030

Bertuzzo, E., Helton, A. M., Hall, R. O., & Battin, T. J. (2017). Scaling of dissolved organic carbon removal in river networks. *Advances in Water Resources*, *110*, 136–146. https://doi.org/10.1016/j.advwatres.2017.10.009

Bishop, K., Buffam, I., Erlandsson, M., Fölster, J., Laudon, H., Seibert, J., & Temnerud, J. (2008). Aqua Incognita: The unknown headwaters. *Hydrological Processes*, *22*(8), 1239–1242. https://doi.org/10.1002/hyp.7049

Blaen, P. J., Khamis, K., Lloyd, C. E. M., Bradley, C., Hannah, D., & Krause, S. (2016). Real-time monitoring of nutrients and dissolved organic matter in rivers: Capturing event dynamics, technological opportunities and future directions. *Science of The Total Environment*, *569–570*, 647–660. https://doi.org/10.1016/j.scitotenv.2016.06.116

Bormann, F. H., & Likens, G. E. (1967). Nutrient cycling. *Science*, *155*(3761), 424–429. https://doi.org/10.1126/science.155.3761.424

Brennan, S. R., Fernandez, D. P., Mackey, G., Cerling, T. E., Bataille, C. P., Bowen, G. J., & Wooller, M. J. (2014). Strontium isotope variation and carbonate versus silicate weathering in rivers from across Alaska: Implications for provenance studies. *Chemical Geology*, *389*, 167–181. https://doi.org/10.1016/j.chemgeo.2014.08.018

Brennan, S. R., Schindler, D. E., Cline, T. J., Walsworth, T. E., Buck, G., & Fernandez, D. P. (2019). Shifting habitat mosaics and fish production across river basins. *Science*, *364*(6442), 783. https://doi.org/10.1126/science.aav4313

Brennan, S. R., Torgersen, C. E., Hollenbeck, J. P., Fernandez, D. P., Jensen, C. K., & Schindler, D. E. (2016). Dendritic network models: Improving isoscapes and quantifying influence of landscape and in-stream processes on strontium isotopes in rivers. *Geophysical Research Letters*, *43*, 5043–5051. https://doi.org/10.1002/2016GL068904

Brennan, S. R., Zimmerman, C. E., Fernandez, D. P., Cerling, T. E., McPhee, M. V., & Wooller, M. J. (2015). Strontium isotopes delineate fine-scale natal origins and migration histories of Pacific salmon. *Science Advances*, *1*(4), e1400124. https://doi.org/10.1126/sciadv.1400124

Buffam, I., Laudon, H., Temnerud, J., Morth, C. M., & Bishop, K. (2007). Landscape-scale variability of acidity and dissolved organic carbon during spring flood in a boreal stream network. *Journal of Geophysical Research*, *112*, G01022. https://doi.org/10.1029/2006JG000218

Callahan, M. K., Whigham, D. F., Rains, M. C., Rains, K. C., King, R. S., Walker, C. M., et al. (2017). Nitrogen subsidies from hillslope alder stands to streamside wetlands and headwater streams, Kenai Peninsula, Alaska. *JAWRA Journal of the American Water Resources Association*, *53*(2), 478–492. https://doi.org/10.1111/1752-1688.12508

Casas-Ruiz, J. P., Catalan, N., Gomez-Gener, L., von Schiller, D., Obrador, B., Kothawala, D. N., et al. (2017). A tale of pipes and reactors: Controls on the in-stream dynamics of dissolved organic matter in rivers. *Limnology and Oceanography*, *62*, S85–S94. https://doi.org/10.1002/lno.10471

Closs, G., Downes, B. J., & Boulton, A. J. (2004). *Freshwater ecology: A scientific introduction*. Malden, MA: Blackwell Pub. Co.

Colpron, M., Nelson, J. L., & Murphy, D. C. (2007). Northern Cordilleran terranes and their interactions through time. *GSA Today*, *17*(4), 4–10. https://doi.org/10.1130/GSAT01704-5A.1

Creed, I. F., McKnight, D. M., Pellerin, B. A., Green, M. B., Bergamaschi, B. A., Aiken, G. R., et al. (2015). The river as a chemostat: Fresh perspectives on dissolved organic matter flowing down the river continuum. *Canadian Journal of Fisheries and Aquatic Sciences*, *72*(8), 1272–1285. https://doi.org/10.1139/cjfas-2014-0400

Cressie, N., Frey, J., Harch, B., & Smith, M. (2006). Spatial prediction on a river network. *Journal of Agricultural, Biological, and Environmental Statistics*, *11*(2), 127–150. https://doi.org/10.1198/108571106x110649

Cressie, N. A. C. (1993). *Statistics for spatial data* (Rev. ed.). New York: Wiley.

Dent, C. L., & Grimm, N. B. (1999). Spatial heterogeneity of stream water nutrient concentrations over successional time. *Ecology*, *80*(7), 2283–2298. https://doi.org/10.1890/0012-9658(1999)080[2283:shoswn]2.0.co;2

Devotta, D. (2017). *The impacts of alder (Alnus spp.) and salmon (Oncorhynchus spp.) on aquatic nutrient dynamics and microbial communities in southwestern Alaska* (PhD dissertation). University of Illinois at Urbana-Champaign.

Dick, J. J., Tetzlaff, D., Birkel, C., & Soulsby, C. (2015). Modelling landscape controls on dissolved organic carbon sources and fluxes to streams. *Biogeochemistry*, *122*(2–3), 361–374. https://doi.org/10.1007/s10533-014-0046-3

Ensign, S. H., & Doyle, M. W. (2006). Nutrient spiraling in streams and river networks. *Journal of Geophysical Research*, *111*, G04009. https://doi.org/10.1029/2005JG000114

Fernald, A. T. (1960). *Geomorphology of the upper Kuskokwim region, Alaska*. Washington, D.C.: United States Department of the Interior, Geological Survey.

Ganio, L. M., Torgersen, C. E., & Gresswell, R. E. (2005). A geostatistical approach for describing spatial pattern in stream networks. *Frontiers in Ecology and the Environment*, *3*(3), 138–144. https://doi.org/10.2307/3868541

Geological Survey, U. S. (2016). *LANDFIRE existing vegetation type, edited by E. R. O. a. S. C. Wildland Fire Science*. Sioux Falls, SD: U.S. Geological Survey.

Gergel, S. E., Turner, M. G., & Kratz, T. K. (1999). Dissolved organic carbon as an indicator of the scale of watershed influence on lakes and rivers. *Ecological Applications*, *9*(4), 1377–1390. https://doi.org/10.1890/1051-0761(1999)009[1377:Docaai]2.0.Co;2

Gooseff, M. N., Bencala, K. E., & Wondzell, S. M. (2008). Solute transport along stream and river networks. In S. P. Rice, A. G. Roy, B. L. Rhoads (Eds.), *River Confluences, Tributaries and the Fluvial Network* (1st ed., pp. 395–417). West Sussex, England: John Wiley & Sons. https://doi.org/10.1002/9780470760383.ch18, https://onlinelibrary.wiley.com/doi/book/10.1002/9780470760383

Granger, S. J., Bol, R., Anthony, S., Owens, P. N., White, S. M., & Haygarth, P. M. (2010). Towards a holistic classification of diffuse agricultural water pollution from intensively managed grasslands on heavy. *The Soil*, *105*(1), 83–115. https://doi.org/10.1016/S0065-2113(10)05003-0

Harms, T. K., Edmonds, J. W., Genet, H., Creed, I. F., Aldred, D., Balser, A., & Jones, J. B. (2016). Catchment influence on nitrate and dissolved organic matter in Alaskan streams across a latitudinal gradient. *Journal of Geophysical Research: Biogeosciences*, *121*, 350–369. https://doi.org/10.1002/2015JG003201

Harms, T. K., & Jones, J. B. (2012). Thaw depth determines reaction and transport of inorganic nitrogen in valley bottom permafrost soils. *Global Change Biology*, *18*(9), 2958–2968. https://doi.org/10.1111/j.1365-2486.2012.02731.x

Hartmann, J., & Moosdorf, N. (2012). The new global lithological map database GLiM: A representation of rock properties at the Earth surface. *Geochemistry, Geophysics, Geosystems*, *13*, Q12004. https://doi.org/10.1029/2012GC004370

Hawkes, J. A., Radoman, N., Bergquist, J., Wallin, M. B., Tranvik, L. J., & Löfgren, S. (2018). Regional diversity of complex dissolved organic matter across forested hemiboreal headwater streams. *Scientific Report-Uk*, *8*(1), 16060. https://doi.org/10.1038/s41598-018-34272-3

Hiatt, D. L., Robbins, C. J., Back, J. A., Kostka, P. K., Doyle, R. D., Walker, C. M., et al. (2017). Catchment-scale alder cover controls nitrogen fixation in boreal headwater streams. *Freshwater Science*, *36*(3), 523–532. https://doi.org/10.1086/692944

Hoeting, J. A., Davis, R. A., Merton, A. A., & Thompson, S. E. (2006). Model selection for geostatistical models. *Ecological Applications*, *16*(1), 87–98. https://doi.org/10.1890/04-0576

Hogan, J. F., & Blum, J. D. (2003). Tracing hydrologic flow paths in a small forested watershed using variations in (87)Sr(/8)6Sr, [Ca]/[Sr], [Ba]/[Sr] and delta O-18. *Water Resources Research*, *39*(10), 1282. https://doi.org/10.1029/2002wr001856

Hunsaker, C. T., & Levine, D. A. (1995). Hierarchical approaches to the study of water quality in rivers: Spatial scale and terrestrial processes are important in developing models to translate research results to management practices. *BioScience*, *45*(3), 193–203. https://doi.org/10.2307/1312558

Ingri, J., Widerlund, A., & Land, M. (2005). Geochemistry of major elements in a pristine boreal river system; Hydrological compartments and flow paths. *Aquatic Geochemistry*, *11*(1), 57–88. https://doi.org/10.1007/s10498-004-2248-0

Intergovernmental Oceanographic Commission (IOC) (1994). *Protocols for the Joint Global Ocean Flux Study (JGOFS) Core Measurements*, *Intergovernmental Oceanographic Commission Manuals and Guides* (Vol. 29, pp. 1–170). Paris, France: UNESCO-IOC. Retrieved from http://hdl.handle.net/11329/220

Jankowski, K. J., & Schindler, D. E. (2019). Watershed geomorphology modifies the sensitivity of aquatic ecosystem metabolism to temperature. *Scientific Report-Uk*, *9*(1), 17619. https://doi.org/10.1038/s41598-019-53703-3

Jorgenson, T., Yoshikawa, K., Kanevskiy, M., Shur, Y., Romanovsky, V., Marchenko, S., et al. (2008). *Permafrost characteristics of Alaska, Fairbanks, AK, United States*. Fairbanks, AK: University of Alaska Fairbanks, Institute of Northern Engineering.

Kaplan, L. A., & Bott, T. L. (1982). Diel fluctuations of doc generated by algae in a Piedmont stream. *Limnology and Oceanography*, *27*(6), 1091–1100. https://doi.org/10.4319/lo.1982.27.6.1091

Kothawala, D. N., Ji, X., Laudon, H., Ågren, A. M., Futter, M. N., Köhler, S. J., & Tranvik, L. J. (2015). The relative influence of land cover, hydrology, and in-stream processing on the composition of dissolved organic matter in boreal streams. *Journal of Geophysical Research: Biogeosciences*, *120*, 1491–1505. https://doi.org/10.1002/2015JG002946

Laudon, H., Berggren, M., Agren, A., Buffam, I., Bishop, K., Grabs, T., et al. (2011). Patterns and dynamics of dissolved organic carbon (DOC) in boreal streams: The role of processes, connectivity, and scaling. *Ecosystems*, *14*(6), 880–893. https://doi.org/10.1007/s10021-011-9452-8

Ledesma, J. L. J., Futter, M. N., Blackburn, M., Lidman, F., Grabs, T., Sponseller, R. A., et al. (2018). Towards an improved conceptualization of riparian zones in boreal Forest headwaters. *Ecosystems*, *21*(2), 297–315. https://doi.org/10.1007/s10021-017-0149-5

Likens, G. E., & Buso, D. C. (2006). Variation in streamwater chemistry throughout the Hubbard Brook Valley. *Biogeochemistry*, *78*(1), 1–30. https://doi.org/10.1007/s10533-005-2024-2

Lintern, A., Webb, J. A., Ryu, D., Liu, S., Bende-Michl, U., Waters, D., et al. (2018). Key factors influencing differences in stream water quality across space. *Wires Water*, *5*(1), e1260. https://doi.org/10.1002/wat2.1260

Loreau, M., Daufresne, T., Gonzalez, A., Gravel, D., Guichard, F., Leroux, S. J., et al. (2013). Unifying sources and sinks in ecology and Earth sciences. *Biological Reviews*, *88*(2), 365–379. https://doi.org/10.1111/brv.12003

Marcé, R., von Schiller, D., Aguilera, R., Martí, E., & Bernal, S. (2018). Contribution of hydrologic opportunity and biogeochemical reactivity to the variability of nutrient retention in river networks. *Global Biogeochemical Cycles*, *32*(3), 376–388. https://doi.org/10.1002/2017GB005677

Matheron, G. (1963). Principles of geostatistics. *Economic Geology and the Bulletin of the Society of Economic Geologists*, *58*(8), 1246–1266. https://doi.org/10.2113/gsecongeo.58.8.1246

McGuire, K. J., Torgersen, C. E., Likens, G. E., Buso, D. C., Lowe, W. H., & Bailey, S. W. (2014). Network analysis reveals multiscale controls on streamwater chemistry. *Proceedings of the National Academy of Sciences*, *111*(19), 7030–7035. https://doi.org/10.1073/pnas.1404820111

Meyer, J. L. (1990). A blackwater perspective on riverine ecosystems. *BioScience*, *40*(9), 643–651. https://doi.org/10.2307/1311431

Meyer, J. L., Mcdowell, W. H., Bott, T. L., Elwood, J. W., Ishizaki, C., Melack, J. M., et al. (1988). Elemental dynamics in streams. *Journal of the North American Benthological Society*, *7*(4), 410–432. https://doi.org/10.2307/1467299

Mineau, M. M., Wollheim, W. M., Buffam, I., Findlay, S. E. G., Hall, R. O. Jr., Hotchkiss, E. R., et al. (2016). Dissolved organic carbon uptake in streams: A review and assessment of reach-scale measurements. *Journal of Geophysical Research: Biogeosciences*, *121*, 2019–2029. https://doi.org/10.1002/2015JG003204

Mulholland, P. J. (1997). Dissolved organic matter concentration and flux in streams. *Journal of the North American Benthological Society*, *16*(1), 131–141. https://doi.org/10.2307/1468246

Mulholland, P. J., Hall, R. O., Sobota, D. J., Dodds, W. K., Findlay, S. E. G., Grimm, N. B., et al. (2009). Nitrate removal in stream ecosystems measured by ^{15}N addition experiments: Denitrification. *Limnology and Oceanography*, *54*, 666–680. https://doi.org/10.4319/lo.2009.54.3.0666

Olea, R. A. (1994). Fundamentals of semivariogram estimation, modeling, and usage. In J. M. Yarus & R. L. Chambers (Eds.), *AAPG computer applications in geology* (pp. 27–35). Tulsa, OK: The American Association of Petroleum Geologists.

Pearson, R. G., Phillips, S. J., Loranty, M. M., Beck, P. S. A., Damoulas, T., Knight, S. J., & Goetz, S. J. (2013). Shifts in Arctic vegetation and associated feedbacks under climate change. *Nature Climate Change*, *3*(7), 673–677. https://doi.org/10.1038/nclimate1858

Peterson, B. J., Wollheim, W. M., Mulholland, P. J., Webster, J. R., Meyer, J. L., Tank, J. L., et al. (2001). Control of nitrogen export from watersheds by headwater streams. *Science*, *292*(5514), 86–90. https://doi.org/10.1126/science.1056874

Peterson, E. E., & Hoef, J. M. V. (2010). A mixed-model moving-average approach to geostatistical modeling in stream networks. *Ecology*, *91*(3), 644–651. https://doi.org/10.1890/08-1668.1

Peterson, E. E., & Hoef, J. M. V. (2014). STARS: An ArcGIS toolset used to calculate the spatial information needed to fit spatial statistical models to stream network data. *Journal of Statistical Software*, *56*(2), 1–17. https://doi.org/10.18637/jss.v056.i02

Peterson, E. E., Merton, A. A., Theobald, D. M., & Urquhart, N. S. (2006). Patterns of spatial autocorrelation in stream water chemistry. *Environmental Monitoring and Assessment*, *121*(1–3), 571–596. https://doi.org/10.1007/s10661-005-9156-7

Peterson, E. E., Theobald, D. M., & Hoef, J. M. V. (2007). Geostatistical modelling on stream networks: Developing valid covariance matrices based on hydrologic distance and stream flow. *Freshwater Biology*, *52*(2), 267–279. https://doi.org/10.1111/j.1365-2427.2006.01686.x

Rieger, S., Schoephorster, D. B., & Furbush, C. E. (1979). *Exploratory soil survey of Alaska*. Washington: U.S. Dept. of Agriculture, Soil Conservation Service.

Rodriguez-Cardona, B., Wymore, A. S., & McDowell, W. H. (2016). DOC:NO_3^- ratios and NO3- uptake in forested headwater streams. *Journal of Geophysical Research: Biogeosciences*, *121*, 205–217. https://doi.org/10.1002/2015JG003146

Rossi, R. E., Mulla, D. J., Journel, A. G., & Franz, E. H. (1992). Geostatistical tools for modeling and interpreting ecological spatial dependence. *Ecological Monographs*, *62*(2), 277–314. https://doi.org/10.2307/2937096

Scenarios Network for Alaska and Arctic Planning (SNAP) (2017). *Historical monthly and derived precipitation products downscaled from CRU TS data via the delta method—2 km, edited*. Fairbanks, Alaska: University of Alaska. Retrieved from http://ckan.snap.uaf.edu/organization/snap

Shaftel, R. S., King, R. S., & Back, J. A. (2012). Alder cover drives nitrogen availability in Kenai lowland headwater streams, Alaska. *Biogeochemistry*, *107*(1–3), 135–148. https://doi.org/10.1007/s10533-010-9541-3

Shogren, A. J., Zarnetske, J. P., Abbott, B. W., Iannucci, F., Frei, R. J., Griffin, N. A., & Bowden, W. B. (2019). Revealing biogeochemical signatures of Arctic landscapes with river chemistry. *Scientific Reports*, *9*, 1. https://doi.org/10.1038/s41598-019-49296-6

Smits, A. P., Schindler, D. E., Holtgrieve, G. W., Jankowski, K. J., & French, D. W. (2017). Watershed geomorphology interacts with precipitation to influence the magnitude and source of CO_2 emissions from Alaskan streams. *Journal of Geophysical Research: Biogeosciences*, *122*, 1903–1921. https://doi.org/10.1002/2017JG003792

Steiger, R. H., & Jager, E. (1977). Subcommission on geochronology—Convention on use of decay constants in geochronology and cosmochronology. *Earth and Planetary Science Letters*, *36*(3), 359–362. https://doi.org/10.1016/0012-821x(77)90060-7

Temnerud, J., Fölster, J., Buffam, I., Laudon, H., Erlandsson, M., & Bishop, K. (2010). Can the distribution of headwater stream chemistry be predicted from downstream observations? *Hydrological Processes*, *24*(16), 2269–2276. https://doi.org/10.1002/hyp.7615

Temnerud, J., Seibert, J., Jansson, M., & Bishop, K. (2007). Spatial variation in discharge and concentrations of organic carbon in a catchment network of boreal streams in northern Sweden. *Journal of Hydrology*, *342*(1), 72–87. https://doi.org/10.1016/j.jhydrol.2007.05.015

Teodoru, C. R., Del Giorgio, P. A., Prairie, Y. T., & Camire, M. (2009). Patterns in pCO_2 in boreal streams and rivers of northern Quebec, Canada. *Global Biogeochemical Cycles*, *23*, Gb2012. https://doi.org/10.1029/2008GB003404

Textor, S. R., Wickland, K. P., Podgorski, D. C., Johnston, S. E., & Spencer, R. G. M. (2019). Dissolved organic carbon turnover in permafrost-influenced watersheds of interior Alaska: Molecular insights and the priming effect. *Frontiers in Earth Science*, *7*(275). https://doi.org/10.3389/feart.2019.00275

U.S. Geological Survey (2017). *Alaska 2 arc-second Digital Elevation Models (DEMs)—USGS National Map 3DEP Downloadable Data Collection*. Reston, Virginia: U.S. Geological Survey.

U.S. Geological Survey (2018). *National Water Information System data available on the World Wide Web (USGS Water Data for the Nation)*. Reston, Virginia: U.S. Geological Survey.

Vannote, R. L., Minshall, G. W., Cummins, K. W., Sedell, J. R., & Cushing, C. E. (1980). River continuum concept. *Canadian Journal of Fisheries and Aquatic Sciences*, *37*(1), 130–137. https://doi.org/10.1139/f80-017

Varanka, S., & Hjort, J. (2016). Spatio-temporal aspects of the environmental factors affecting water quality in boreal rivers. *Environmental Earth Sciences*, *76*(1), 1–13. https://doi.org/10.1007/s12665-016-6338-2

Varanka, S., Hjort, J., & Luoto, M. (2015). Geomorphological factors predict water quality in boreal rivers. *Earth Surface Processes and Landforms*, *40*(15), 1989–1999. https://doi.org/10.1002/esp.3601

Ver Hoef, J., Peterson, E., Clifford, D., & Shah, R. (2014). SSN: An R package for spatial statistical modeling on stream networks. *Journal of Statistical Software*, *56*(3). https://doi.org/10.18637/jss.v056.i03

Ver Hoef, J. M., Peterson, E., & Theobald, D. (2006). Spatial statistical models that use flow and stream distance. *Environmental and Ecological Statistics*, *13*(4), 449–464. https://doi.org/10.1007/s10651-006-0022-8

Ver Hoef, J. M., & Peterson, E. E. (2010). A moving average approach for spatial statistical models of stream networks. *Journal of the American Statistical Association*, *105*(489), 6–18. https://doi.org/10.1198/jasa.2009.ap08248

Walker, C. M., King, R. S., Whigham, D. F., & Baird, S. J. (2012). Landscape and wetland influences on headwater stream chemistry in the Kenai lowlands, Alaska. *Wetlands*, *32*(2), 301–310. https://doi.org/10.1007/s13157-011-0260-x

Webster, J. R., & Patten, B. C. (1979). Effects of watershed perturbation on stream potassium and calcium dynamics. *Ecological Monographs*, *49*(1), 51–72. https://doi.org/10.2307/1942572

Weyhenmeyer, G. A., & Conley, D. J. (2017). Large differences between carbon and nutrient loss rates along the land to ocean aquatic continuum—Implications for energy:nutrient ratios at downstream sites. *Limnology and Oceanography*, *62*(S1), S183–S193. https://doi.org/10.1002/lno.10589

Weyhenmeyer, G. A., Froberg, M., Karltun, E., Khalili, M., Kothawala, D., Temnerud, J., & Tranvik, L. J. (2012). Selective decay of terrestrial organic carbon during transport from land to sea. *Global Change Biology*, *18*(1), 349–355. https://doi.org/10.1111/j.1365-2486.2011.02544.x

Wickland, K. P., Waldrop, M. P., Aiken, G. R., Koch, J. C., Jorgenson, M. T., & Striegl, R. G. (2018). Dissolved organic carbon and nitrogen release from boreal Holocene permafrost and seasonally frozen soils of Alaska. *Environmental Research Letters*, *13*(6), 1–11. https://doi.org/10.1088/1748-9326/aac4ad

Wiens, J. A. (1989). Spatial scaling in ecology. *Functional Ecology*, *3*(4), 385–397. https://doi.org/10.2307/2389612

Winterdahl, M., Laudon, H., Lyon, S. W., Pers, C., & Bishop, K. (2016). Sensitivity of stream dissolved organic carbon to temperature and discharge: Implications of future climates. *Journal of Geophysical Research: Biogeosciences*, *121*, 126–144. https://doi.org/10.1002/2015JG002922

Wohl, E., Hall, R. O. Jr., Lininger, K. B., Sutfin, N. A., & Walters, D. M. (2017). Carbon dynamics of river corridors and the effects of human alterations. *Ecological Monographs*, *87*(3), 379–409. https://doi.org/10.1002/ecm.1261

Zimmer, M. A., Bailey, S. W., McGuire, K. J., & Bullen, T. D. (2013). Fine scale variations of surface water chemistry in an ephemeral to perennial drainage network. *Hydrological Processes*, *27*(24), 3438–3451. https://doi.org/10.1002/hyp.9449

References From the Supporting Information

Manley, W., & Kaufman, D. (2002). *Alaska PaleoGlacier Atlas*, *A Geospatial Compilation of Pleistocene Glacier Extents*. University of Colorado: Institute of Arctic and Alpine Research (INSTAAR). Retrieved from http://instaar.colorado.edu/QGISL/ak_paleoglacier_atlas/

Soil Survey Staff, Natural Resources Conservation Service, and United States Department of Agriculture (2016). *USDA-NRCS Soil Survey Geographic (SSURGO)*, edited by Forth Worth, TX: USDA/NRCS National Geospatial Center of Excellence.